

Laser propagation in dense magnetized plasma

S. X. Luan,¹ W. Yu,¹ F. Y. Li,² D. Wu¹, Z. M. Sheng,^{2,3} M. Y. Yu,^{4,5} and J. Zhang³

¹ State Key Laboratory of High Field Laser Physics, Shanghai Institute of Optics and Fine Mechanics, Chinese Academy of Science, Shanghai 201800, China.

² SUPA, Department of Physics, University of Strathclyde, Glasgow G4 0NG, UK

³ Laboratory for Laser Plasmas and Department of Physics and Astronomy, Shanghai Jiao Tong University, Shanghai 200240, China

⁴ Institute of Fusion Theory and Simulation, Zhejiang University, Hangzhou 310027, China

⁵ Institute for Theoretical Physics I, Ruhr University, Bochum, D-44780 Germany.

Abstract

A right-hand circularly polarized electromagnetic wave can propagate in a sufficiently magnetized plasma of any density without cutoff in the so-called whistler mode. With the recent realization of tens-kilotesla magnetic fields, laser propagation in highly magnetized high-density plasmas has become of practical interest, especially for heating plasmas to high energy density and igniting fusion targets. In this paper, the whistler regime of laser-plasma interaction is discussed. It is shown that moderately intense right-hand circularly polarized laser light can enter and propagate in high-density plasma and heat it efficiently because of the significantly reduced wave length and speed.

PACS numbers: 52.57.Kk, 52.38.-r, 52.65.Rr, 52.65.Ww

I. Introduction

Propagation and interactions of electromagnetic (EM) waves in weakly-magnetized and weakly-ionized plasmas have been studied extensively since the late 1940s because of their relevance to radio and radar wave transmission in the Earth's ionosphere as well as for plasma production in many laboratory and industrial plasma devices [1-8]. The wave propagation properties depend strongly on the EM wave polarization, the plasma density, and the magnetic field strength and orientation. For circularly polarized (CP) EM waves propagating along the external magnetic field B_0 , the linear plasma dielectric constant can be written as [2]

$\epsilon_{B\mp} = 1 - n / (1 \mp B_0)$, where (following the CMA-diagram parameters, which turn out to be particularly convenient for laser-plasma interaction studies) $n = \omega_p^2 / \omega^2$ is the electron density normalized by the classical (i.e., for unmagnetized plasma) critical density $n_c = m_e \omega^2 / 4\pi e^2$, $B_0 = \omega_c / \omega$ is the external magnetic field strength normalized by $m_e \omega c / e$, $-e$ and m_e are the electron charge and mass, respectively, and ω , ω_p , and ω_c are the EM wave, electron plasma, and cyclotron frequencies, respectively. The minus and plus signs denote right-hand (RH) and left-hand (LH) CP waves, respectively. As mentioned, earlier studies have mainly been on low-frequency EM wave propagation in weakly magnetized plasmas, such as that of the radio frequencies (KHz—MHz) and the Earth's field (tens μT) [1-6]. The RHCP EM wave in the whistler regime $B_0 > 1$ has been of particular interest because of its distinctive features and effect on radio communication, as well as usefulness in the production and heating of dense laboratory and industrial plasmas, such as that of the helicon plasma device and thruster [9-12]. For the much higher frequency light waves, the whistler regime is also realized around cosmic bodies such as pulsars and magnetars [13], where extremely strong (TT to PT) magnetic fields can exist [14]. However, the whistler regime for laser light propagation in laboratory plasma has been mostly ignored in view of the limited strength of available magnetic fields. Recent advances in high magnetic field production and discovery of self-generated

tens-kilotesla magnetic fields in ultrahigh-intensity laser interaction with matter have made this regime within reach [15-18]. For example, for the $1.06\mu\text{m}$ Nd-glass laser, $B_0 \geq 1$ corresponds to a magnetic field ≥ 9 kilotesla, and for the $10.6\mu\text{m}$ CO₂ laser the corresponding magnetic field is an order of magnitude less [19, 20]. It is therefore timely to investigate laser-plasma interaction in the whistler regime, where a moderately intense (say 10^{15} W/cm²) long-pulse RHCP laser can ionize high-density matter as well as propagate deep into the resulting plasma if the latter is sufficiently magnetized. Such a scenario is especially desirable for inertial confinement fusion, where intense laser light should propagate deep into the fuel pellet [21].

In this paper, we consider the propagation of RHCP laser light in the whistler regime in a highly overdense magnetized plasma slab by particle-in-cell (PIC) simulation. To avoid excitation of the many waves and their complex propagation characteristics that can occur in a magnetized plasma, the slab is of uniform density and the magnetic field is along the direction of the laser. In order to avoid strong nonlinear effects, the latter is also of moderate intensity. As expected, a large fraction of the incident laser can enter and propagate deep into the plasma without encountering cutoff. It is shown that electron-ion collisions can efficiently convert the laser energy into that of the plasma electrons, so that dense magnetized plasmas can be heated directly by the laser without being structurally altered.

II. The interaction model

It is instructive to briefly review the linear theory of CP light propagation along the embedded magnetic field $\mathbf{B}_0 = B_0 \hat{z}$ in uniform overdense cold plasma located in $z \geq 0$. The laser electric field can be written as [2] $\mathbf{E} = E \exp(-i\omega t + ik_z z)(\hat{x} \pm i\hat{y})$, where k_z and ω are the wave vector and frequency, respectively, which satisfy the linear dispersion relation $k_z^2 = \varepsilon_{Bm}$, with k_z normalized by ω/c . Accordingly, we have $k_z^2 = 1$ in the vacuum ($z < 0$)

and $k_z^2 = \epsilon_{B\mp}$ in the plasma. The solution of the wave equation for the normalized electric field $a = eE / m\omega_0 c$ is then $a = a_0 e^{iz} + a_R e^{-iz}$ for the incident and reflected light in the vacuum, and $a = a_T e^{ik_T z}$, where $k_T = \sqrt{\epsilon_{B\mp}}$, for the transmitted light in the plasma. The subscripts 0, R, and T denote the incident, reflected (backward propagating), and transmitted quantities, respectively. In view of causality, there is no backward propagating light in the *uniform* plasma. The boundary condition that a and $\partial_z a$ be continuous at $z=0$ [22] leads to $a_R = a_0(1-k_T)/(1+k_T)$, so that the reflectivity is

$$\mathfrak{R} \equiv (a_R / a_0)^2 = (1-k_T)^2 / (1+k_T)^2. \quad (1)$$

Figure 1 shows the incident (blue solid curves) and reflected (red dashed curves) EM waves in the vacuum, and the transmitted (black dash-dot curves) wave in the dense plasma for LHCP (a) and RHCP (b) EM wave trains, as given by the linear theory for $n_0 = 50$ and $B_0 = 8$. The green dotted curves are from superposition of the incident and the reflected waves in the front vacuum region. We see that since the plasma density is higher than the left cutoff density $n_{Lc} = 1+B_0$, a LHCP EM wave can only penetrate about a skin depth ($d/\lambda_0 = |\epsilon_{B+}|^{-1/2} \sim 0.47$) into the plasma. It is then reflected back into the front vacuum region. In contrast, since there is no cut-off for the RHCP EM wave for $B_0 > 1$, a considerable fraction of the incident wave is transmitted and can propagate into the overdense magnetized plasma. It is of interest to note that the transmitted wave is blue shifted, having a reduced wavelength $\lambda_T = 2\pi / k_T = 2\pi\epsilon_{B-}^{-1/2} \sim 0.35 \times 2\pi$, or 0.35 times that of the incident wave. We recall that for EM waves propagating into unmagnetized underdense plasma (or LHCP waves at above the left cutoff frequency propagating into magnetized overdense plasma [2]), the transmitted waves are red shifted and their phase velocity increases. Figure 1(c) and 1(d) give the reflectivity \mathfrak{R} versus the plasma density and external magnetic field. The solid and dashed curves are for RHCP and LHCP EM waves, respectively. As expected, the LHCP light is totally reflected since in the regime

considered here ($n_0 = 10-100$ and $1 < B_0 < 8$) the plasma density is higher than that ($n_{Lc} = 1 + B_0$) of the left cutoff, but a large part of the RHCP laser can enter and propagate in the dense plasma. One can also see that the reflectivity decreases with increase of B_0 . The results from one-dimensional PIC simulation for laser intensity $a_0 = 0.1$ (weakly nonlinear) and pulse duration $\tau = 50T_0$ are also shown, and one can see that they agree well with that from the linear theory. Here the propagation of RHCP laser light into the overdense plasma is a basically a linear effect, and is significantly different from the nonlinear propagation effects such as self-transparency, tunneling, snow-plowing, etc. [23-34] associated with intense laser interaction with the plasma. In the latter, both the laser and the plasma are often strongly modified.

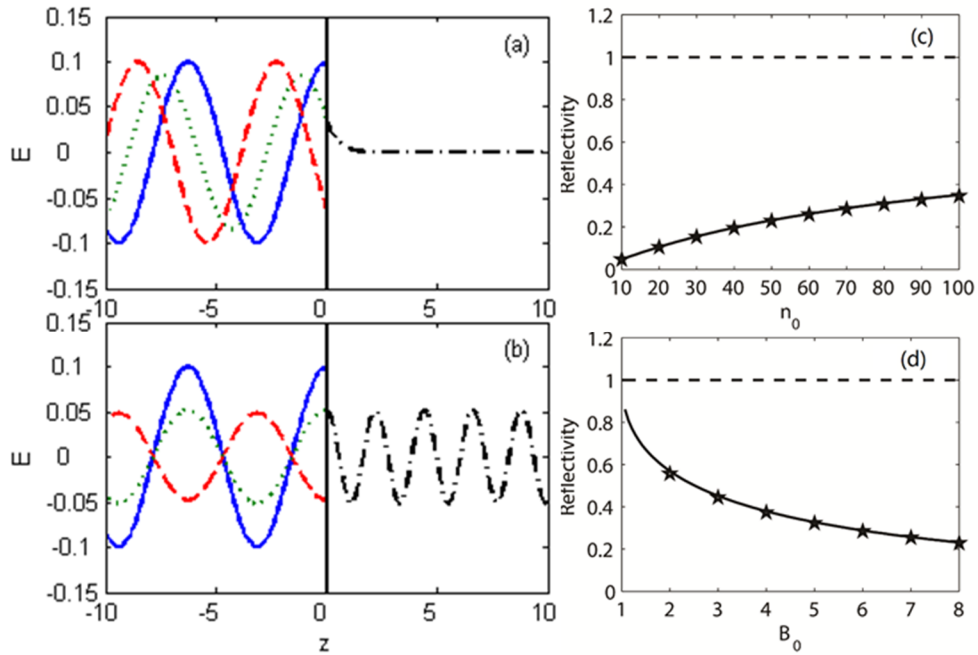


Fig. 1 (Color online). Propagation of (a) left-hand and (b) right-hand circularly polarized electromagnetic wave in an $n_0 = 50$ plasma with $B_0 = 8$. The vacuum-plasma boundary is at $z = 0$. The solid blue and dashed red curves represent the incident and reflected waves, and the dotted dark green curves represent their sum. The black dashed-dotted curves represent the transmitted light. Also

shown are the reflectivity as function of (c) plasma density n_0 and (d) external magnetic field strength B_0 , for LHCP (dashed curve) and RHCP (solid curve) light. The stars are from one-dimensional PIC simulation for laser with intensity $a_0 = 0.1$ and pulse duration $\tau = 50T_0$. One can see that the LHCP wave in this parameter regime is totally reflected.

III. PIC simulation results

Next we investigate the propagation of laser pulse into highly magnetized dense plasmas using two-dimensional (2D) PIC simulation. The laser is normally incident from the left vacuum region into a homogeneous plasma slab located in $z \geq 20\lambda_0$. Its strength parameter and spot size are $a_0 = 0.1$ and $b = 3\lambda_0$, respectively. The duration of the long laser pulse is $\tau = 500T_0$, where T_0 is the light-wave period. The laser is moderately nonlinear, so that the plasma would not be strongly modified. The plasma density is $n = 50$, the strength of the external magnetic field is $B_0 = 8$, and the ion-electron mass ratio is 1836. Free boundary conditions are used for all sides of the simulation box.

Figure 2 shows the EM field energy density $E^2 + B^2$ at $t = 90T_0$ for the (a) LH and (b) RH CP laser pulse. One can see that the incident LHCP pulse is totally reflected since its frequency is below the left cutoff frequency [2] $\omega_{Lc} = \frac{1}{2}[-B_0 + (B_0^2 + 4n)^{1/2}] \sim 4.12$. The RHCP laser pulse is partially reflected, but the transmitted light can propagate deep into the dense plasma.

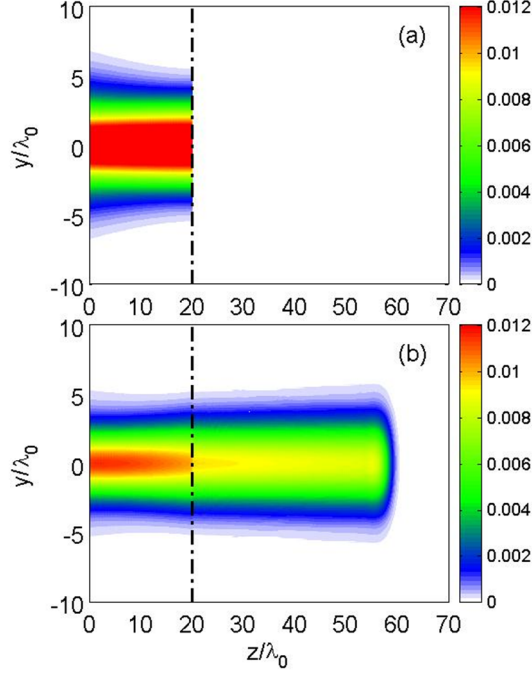


Fig. 2 (Color online). The EM field energy density $E^2 + B^2$ distribution at $t = 90T_0$ for (a) LHCP and (b) RHCP laser pulse. The interaction parameters are $a_L = 0.1$, $b = 3\lambda$, $n_0 = 50$, and $\tau = 500T_0$. The external magnetic field is $B_0 = 8$. One can clearly see that, similar to the prediction of the 1D linear theory and simulation, the LHCP laser is reflected, and a part of the RHCP laser is entering the slab.

Since here we are considering moderately intense, long-pulse, and short-wavelength light propagation in strongly magnetized homogeneous dense cold plasma in the whistler regime, the laser light does not encounter resonance or cutoff. Accordingly, energy transfer from light to plasma is mainly by collisions, or inverse bremsstrahlung. Accordingly, we include in the PIC simulation the effect of collisions using the code OSIRIS [35]. The laser and plasma parameters are the same as that in Fig. 1, except that (in order to save computational resource) here we use a laser with lower intensity, namely $a_L = 0.04$, but the corresponding wave electric field is still above that needed for ionization of solids [36,37]. Both the electrons and ions have the initial temperature 0.1 keV. Electron-ion collisions heat the electrons that are rapidly oscillating in the short-wavelength light field by randomizing their motion. The Coulomb logarithm is

evaluated at the local plasma conditions, so that the modification of the collision frequency due to electron temperature increase is self-consistently included. Figure 4 shows the evolution of the EM energy flux and electron kinetic energy along the laser propagation direction, together with the electron energy spectra. We can see that the transmitted laser light attenuates as it propagates, eventually almost all its energy is converted into electron kinetic energy. The electron temperature increases to ~ 0.78 keV within about ~ 2 ps. Their energy spectrum also broadens with time. One can also see that even though the incident laser is not of high intensity and collisional damping is strong, a small fraction of the transmitted laser light can still penetrate through the slab. A small number of electrons are also driven out into the backside vacuum by the small but finite ponderomotive force. The result here suggests that in the presence of strong magnetic field one can heat cold dense plasma directly by moderately intense long-pulse laser. The process should therefore be useful for creating high energy density plasma with moderate intensity long-pulse laser.

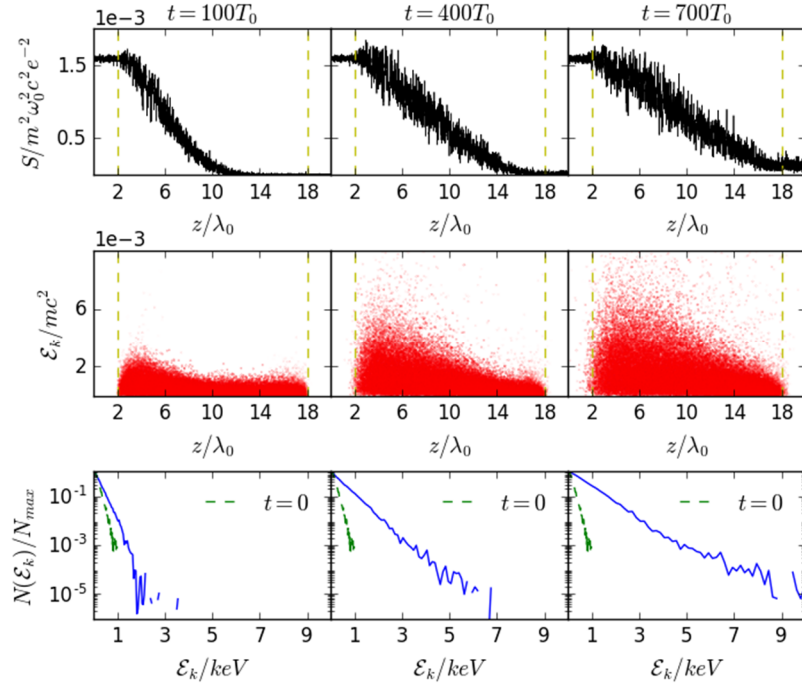


Fig. 3 (Color online). Upper row: EM energy flux S in the forward direction, middle row: electron kinetic energy \mathcal{E}_k , bottom row: electron kinetic energy spectrum $N(\mathcal{E}_k)$, at $t=100T_0$, $400T_0$ and $700T_0$, where T_0 is the laser light period. The vertical dashed lines in the first two rows define the plasma slab, and the green dashed

curves in the bottom row are for the initial electron energy spectra. One can see that the laser attenuates as it propagates in the plasma, with its energy transferred to the electrons, which are heated.

IV. Conclusion

We have considered the transmission into and propagation of a long moderately intense RHCP laser pulse in a much-above-critical-density ($n \gg 1$) strongly-magnetized ($B_0 > 1$) plasma. It is verified that the laser light can propagate along the magnetic field for long distances without cutoff or resonance. Since the light wave in this regime has low phase velocity and short wavelength, it can efficiently heat the plasma via electron-ion collisions, making possible nondestructive laser heating of very dense plasmas in applications such as creating high energy density plasma and inertial confinement fusion. It should be noted that if the phase velocity of the EM wave become too low, ion response could play a role in the light wave propagation characteristics, which could be significantly modified. However, such a regime can be reached only if the plasma density and/or embedded magnetic field are extremely high.

For the purpose of demonstration and comparison with the existing theoretical results, we have considered a particularly simple interaction model and a RHCP incident laser. As mentioned, a LHCP laser can also enter into a strongly magnetized overdense plasma if the plasma density is less than that of the left cutoff, or $n < n_{lc} (=1+B_0)$. Moreover, laser pulses in directions other than along the external magnetic field can also enter a dense plasma. For example, in a highly magnetized overdense plasma a light pulse can propagate perpendicular or other angles to the embedded magnetic field as extraordinary or mixed waves [1,38,39]. In view of the frequent detection of ultra-strong self-generated magnetic fields in the interaction of intense lasers with solid matter, their investigation should be relevant for the interpretation of many experimental results. However, in general, the propagation and interaction behavior of intense EM waves in magnetized plasmas are rather complex even in the linear limit [1,2],

especially when the plasma density and magnetic field are highly inhomogeneous, so that intensive numerical simulation would be required for their investigation. Finally, it may be of interest to point out that kilo-tesla magnetic fields have recently been used for efficiently guiding relativistic electron beams in dense plasma [40].

ACKNOWLEDGMENTS

This work was supported by the National Basic Research Program of China (2013CBA01504 and 2011CB808104), the National Natural Science Foundation of China (11304331, 11374262, 11421064, and 11475147), and the Open Fund of the State Key Laboratory of High Field Laser Physics at SIOM. The numerical simulations have partly been performed at the ARCHER computing service through the Plasma HEC Consortium EPSRC grant number EP/L000237/1. FYL and ZMS would like to acknowledge the OSIRIS Consortium, consisting of UCLA and IST (Lisbon, Portugal), for providing access to the OSIRIS 2.0 framework.

REFERENCES

1. P. C. Clemmow and J. P. Dougherty, *Electrodynamics of Particles and Plasmas* (Addison-Wesley, Reading, Mass, 1969).
2. F. F. Chen, *Introduction to Plasma Physics and Controlled Fusion*, Vol 1: Plasma Physics, 2nd ed. (Plenum Press, 1984).
3. G. V. Khazanov, A. A. Tel'nikhin, and T. K. Kronberg, *Plasma Phys. Controlled Fusion* **49**, 447 (2007).
4. A. V. Artemyev, A. A. Vasiliev, D. Mourenas, O. V. Agapitov, and V. V. Krasnoselskikh, *Phys. Plasmas* **20**, 122901 (2013).
5. K. H. Lee, Y. Omura, and L. C. Lee, *Phys. Plasmas* **20**, 112901 (2013).
6. P. H. Yoon, V. S. Pandey, and D. H. Lee, *Phys. Plasmas* **20**, 112902 (2013).

7. S. Sen, M. A. Varshney, and D. Varshney, *High Energy Density Phys.* **11**, 80 (2014).
8. N. Wadhvani, P. Kumar, and P. Jha, *Phys. Plasmas* **9**, 263 (2002).
9. R. W. Boswell, *Plasma Phys. Controlled Fusion* **26**, 1147 (1984).
10. F. F. Chen, *Plasma Phys. Controlled Fusion* **33**, 339 (1991).
11. M. A. Lieberman and A. J. Lichtenberg, *Principles of Plasma Discharges and Materials Processing* (Wiley, New York, 1994).
12. K. Takahashi, A. Chiba, A. Komuro, and A. Ando, *Phys. Rev. Lett.* **114**, 195001 (2015)
13. V. Canuto and H. Y. Chiu, *Space Sci. Rev.* **12**, 3 (1971).
14. R.A. Treumann, W. Baumjohann, and A. Balogh, *Front. Phys.* (2014).
doi:10.3389/fphy.2014.00059
15. Z. M. Sheng and J. Meyer-ter-Vehn, *Phys. Rev. E* **54**, 1833 (1996).
16. J. P. Knauer, O. V. Gotchev, P. Y. Chang, D. D. Meyerhofer, O. Polomarov, R. Betti, J. A. Frenje, C. K. Li, M. J. E. Manuel, R. D. Petrasso, J. R. Rygg, and F. H. Seguin, *Phys. Plasmas* **17**, 056318 (2010).
17. H. Yoneda, T. Namiki, A. Nishida, R. Kodama, Y. Sakawa, Y. Kuramitsu, T. Morita, K. Nishio, and T. Ide, *Phys. Rev. Lett.* **109**, 125004 (2012).
18. U. Wagner, M. Tatarakis, A. Gopal, F. N. Beg, E. L. Clark, A. E. Dangor, R. G. Evans, M. G. Haines, S. P. D. Mangles, P. A. Norreys, M. S. Wei, M. Zepf, and K. Krushelnick, *Phys. Rev. E* **70**, 026401 (2004).
19. P. Y. Chang, G. Fiksel, M. Hohenberger, J. P. Knauer, R. Betti, F. J. Marshall, D. D. Meyerhofer, F. H. Seguin, and R. D. Petrasso, *Phys. Rev. Lett.* **107**, 035006 (2011).
20. S. Fujioka, Z. Zhang, K. Ishihara, K. Shigemori, Y. Hironaka, T. Johzaki, A. Sunahare, N. Yamamoto, H. Nakashima, T. Watanabe et al., *Sci. Rep.* **3**, 1170 (2013).
21. S. Atzeni and J. Meyer-ter-Vehn, *The Physics of Inertial Fusion* (Oxford University Press, Oxford, 2004)
22. J. D. Jackson, *Classical electrodynamics*, 3rd ed. (Wiley, New York, 1998).
23. S. M. Weng, M. Murakami, P. Mulser, and Z. M. Sheng, *New J. Phys.* **14**, 063026 (2012).
24. P. W. Kaw and J. M. Dawson, *Phys. Fluids* **13**, 472 (1970).

25. S. M. Weng, P. Mulser, and Z. M. Sheng, *Phys. Plasmas* **19**, 022705 (2012).
26. G. Shvets and J. S. Wurtele, *Phys. Rev. Lett.* **73**, 3540 (1994).
27. P. Sprangle, J. Krall, and E. Esarey, *Phys. Rev. Lett.* **73**, 3544 (1994).
28. Ya. B. Zel'dovich and Yu. P. Raizer, *Physics of Shock Waves and High-Temperature Hydrodynamic Phenomena* (Academic, New York, 1967).
29. C. J. McKinstrie and E. A. Startsev, *Phys. Rev. E* **54**, R1070 (1996).
30. E. A. Startsev and C. J. McKinstrie, *Phys. Plasmas* **10**, 2552 (2003).
31. C. Du and Z. Xu, *Phys. Plasmas* **7**, 1582 (2000).
32. M. Y. Yu, W. Yu, Z. Y. Chen, J. Zang, Y. Yin, P. X. Lu, L. H. Cao, and Z. Z. Xu, *Phys. Plasmas* **10**, 2468 (2003).
33. M. Eloy, A. Guerreiro, J. T. Mendonça, and R. Bingham, *J. Plasma Phys.* **73**, 635 (2007).
34. V. I. Geyko, G. M. Fraiman, I. Y. Dodin, and N. J. Fisch, *Phys. Rev. E* **80**, 036404 (2009).
35. R. Fonseca et al., *Proceedings of the Second International Conference on Computational Science—ICCS, Amsterdam, 2002, Lecture Notes in Computer Science, Vol. 2331* (Springer, Berlin, 2002), p. 342.
36. G. Ecker and W. Kroll, *Phys. Fluids* **6**, 62 (1963).
37. R. E. Bruce and F. C. Todd, *Proc. Okla. Acad. Sci.* **44**, 95 (1963).
http://digital.library.okstate.edu/oas/oas_pdf/v44/p95_102.pdf
38. V. Artemyev, A. A. Vasiliev, D. Mourenas, O. V. Agapitov, and V. V. Krasnoselskikh, *Phys. Plasmas* **20**, 122901 (2013).
39. B. Van Compernelle, X. An, J. Bortnik, R. M. Thorne, P. Pribyl, and W. Gekelman, *Phys. Rev. Lett.* **114**, 245002 (2015); *ibid.*, **117**, 059901 (2016).
40. S. Fujioka, Y. Arikawa, S. Kojima, T. Johzaki, H. Nagatomo, H. Sawada, S. H. Lee, T. Shiroto, N. Ohnishi, A. Morace, et al. *Phys. Plasmas* **23** 056308 (2016).

